CT-monitored Percutaneous Cryoablation in a Pig Liver Model: Pilot Study[1]

Fred T. Lee, Jr, MD
Susan G. Chosy, BS
Peter J. Littrup, MD
Thomas F. Warner, MD
Janet E. Kuhlman, MD
David M. Mahvi, MD

Index terms:
Computed tomography (CT), guidance, 761.12111
Cryotherapy, 761.30
Liver, interventional procedures, 761.1267
Liver neoplasms, CT, 761.12111, 761.30

Radiology 1999; 211:687–692

[1] From the Departments of Radiology (F.T.L., S.G.C., J.E.K.), Pathology (T.F.W.), and Surgery (D.M.M.), University of Wisconsin, E3/311 CSC, 600 Highland Ave, Madison, WI 53792; and the Department of Radiology, Wayne State University, Detroit, Mich (P.J.L.). Received May 7, 1998; revision requested July 7; revision received August 7; accepted November 6. F.T.L., P.J.L., and D.M.M. supported in part by Endocare, Irvine, Calif. F.T.L. supported by the RSNA Research and Education Foundation as a GE/RSNA Scholar. **Address reprint requests to** F.T.L. (e-mail: *ftlee@facstaff.wisc.edu*).

F.T.L., P.J.L., and D.M.M. are ad hoc consultants for Endocare.

Author contributions:
Guarantors of integrity of entire study, F.T.L., S.G.C.; study concepts, F.T.L., P.J.L., D.M.M.; study design, F.T.L., S.G.C., J.E.K., D.M.M.; definition of intellectual content, F.T.L., S.G.C., T.F.W., D.M.M.; literature research, S.G.C.; experimental studies, F.T.L., S.G.C., P.J.L., T.F.W.; data acquisition, F.T.L., S.G.C., P.J.L., T.F.W.; data analysis, F.T.L., S.G.C.; statistical analysis, S.G.C.; manuscript preparation, F.T.L., S.G.C., P.J.L., T.F.W.; manuscript editing and review, S.G.C., P.J.L., T.F.W., J.E.K., D.M.M.

PURPOSE: To determine the safety and feasibility of percutaneous cryoablation with computed tomographic (CT) guidance in a pig liver model.

MATERIALS AND METHODS: Nine angiographic balloons (mean diameter, 9 mm) were placed in the livers of seven domestic pigs (mean weight, 30.0 kg ± 14.0 [SD]) as tumor-mimicking lesions. By using ultrasonographic and CT guidance, two 2.4- or 3.0-mm cryoprobes were placed flanking the balloon, and a 15–20-minute freezing process was performed. Hemostasis was achieved by placing absorbable cellulose fabric down the probe tract. After 24–96 hours, animals were sacrificed, and their livers were removed and were sectioned axially at 5-mm intervals for comparison with CT images.

RESULTS: All animals survived the procedure without complication. No serious hemorrhage was found in any case. Ice balls were readily visualized at CT because they appeared as areas of decreased attenuation (1.0 HU ± 20.7) when compared with areas of normal liver (48.2 HU ± 6.3, $P < .05$). The mean ablative margin was 1.7 cm, and only one of nine cases, the one with probe failure, had a positive margin. Beam-hardening artifact from the metal probes was present but did not interfere with the procedure. Ice-ball size and shape corresponded closely to the area of necrosis determined at histopathologic analysis.

CONCLUSION: CT-monitored percutaneous cryoablation is feasible and safe in this pig liver model.

Over 56,000 deaths from colorectal carcinoma are anticipated in the United States in 1999 (1). Almost all of these patients die of isolated hepatic disease or of a combination of hepatic and other distant metastases (2,3). Although hepatic metastases are a sign of systemic disease for most tumor types, approximately 10%–20% of patients with colorectal carcinoma metastases limited to the liver have carcinomas that are still potentially curable by hepatic resection (4). Removal of all macroscopic tumor in these patients results in long-term survival rates of 30%–40% for patients undergoing resection. This is substantial when compared with the very limited benefits of chemotherapy (2,4,5). Liver resection for curative intent has been limited by the number and size of metastases, by the presence of tumor in unresectable locations, by the presence of tumor in multiple segments, and by underlying conditions or illnesses that render carcinoma inoperable (6,7).

Various targeted ablation techniques have been introduced in attempts to overcome the limitations of hepatic resection and to increase the number of patients eligible for tumor removal or tumor ablation. Technologies that have been investigated include ethanol injection, radio-frequency ablation, laser photocoagulation, high-intensity focused ultrasound, and cryoablation (8–17).

Although some of these techniques have shown promise, each has considerable limitations. Ethanol injection does not adequately ablate metastases because of the uncontrolled diffusion of ethanol away from the injection site (8). Radio-frequency ablation involves a rapidly alternating current to cause tissue heating and, ultimately, cell death. Although bleeding is not common in patients who undergo this procedure, questions remain about the reliability of radio-frequency ablation to cause cell death within a targeted zone (9–11). This same limitation applies to laser photocoagulation and to high-intensity focused ultrasound (12–14).

In addition, the use of real-time imaging guidance for radio-frequency ablation, laser photocoagulation, and high-intensity focused ultrasound to accurately predict the degree of tissue necrosis has been a problem (10–15). Despite these limitations, considerable interest in radio-frequency ablation continues because of its potential percutaneous application.

Of all the targeted ablation techniques, cryoablation is the most widely used and accepted because it produces ice balls of consistent size and shape, and it reliably causes cell death within the cryolesion (16–20). However, the technology has been traditionally limited to intraoperative use because of the large probes that can cause serious bleeding when removed (18,21).

The purpose of this study was to evaluate the safety and feasibility of percutaneous cryoablation with computed tomographic (CT) guidance. We investigated whether serious bleeding could be avoided by using the Seldinger technique and by embolizing the probe tract, whether CT adequately permits estimation of the amount and the location of tissue necrosis caused by the freezing process, and whether adequate ablation margins can be obtained by using this technique in a pig model.

MATERIALS AND METHODS

Animals and Balloon Placement

Preapproval by the Institutional Animal Care and Use Committee, University of Wisconsin, Madison, was obtained for all experiments described in this article. All procedures and imaging were performed with the animals under general anesthesia. Induction was achieved by using an intramuscular injection of tiletamine hydrochloride and zolazepam hydrochloride (Telazol; Fort Dodge Animal Health, Iowa) and xylazine hydrochloride (Xyla-Ject; Phoenix Pharmaceuticals, St Joseph, Mo). The animals were then intubated and were administered inhaled halothane (Fluothane; Halocarbon Laboratories, River Edge, NJ).

Once adequate anesthesia was achieved, nine angiographic balloons (Goldvalve; Laboratoires Nycomed, Paris, France) were placed percutaneously to mimic tumors in the livers of seven domestic pigs (mean weight, 30.0 kg ± 14.0 [SD]) with ultrasonographic (US) guidance (model SSD-2000; Aloka Ultrasound, Wallingford, Conn). This was accomplished by puncturing the liver with a 14-gauge needle and by placing a 3.0-F catheter (Tracker-18; Boston Scientific Target, Natick, Mass), with the balloon seated at the tip, into the hepatic parenchyma. Balloons were inflated with approximately 1.0 mL of liquid agar with a gelling point of 42°C (Type V high-gelling agarose; Sigma Chemical, St Louis, Mo). The catheter and needle were then withdrawn to leave the balloon in place to mimic a hepatic lesion.

Cryoablation with CT Guidance

Animals were transported to the CT scanner (HiQ; GE Medical Systems, Milwaukee, Wis), and two 18-gauge needles were placed with US guidance to flank each balloon. By using the Seldinger technique, the tracts were dilated, and the guide wires were exchanged for sheath-dilator combinations (Onik-Cohen percutaneous access kits; Cook, Bloomington, Ind) through which 2.4-mm ($n = 3$) or 3.0-mm ($n = 6$) cryoprobes were placed (Fig 1). Limited CT scanning was performed (5-mm sections, 1:1 pitch) through the lesion and the cryoprobes to confirm proper positioning. If necessary, adjustments in the position of the cryoprobes were made by using a combination of CT and US guidance. In one animal, 1.0 L of normal saline was instilled into the abdomen as a buffer between the ice ball and the anterior abdominal wall (Fig 1).

The cryoablation unit used for this study was an argon gas–based system (Cryocare; Endocare, Irvine, Calif). Argon was cycled through the cryoprobes for 15 minutes (20 minutes in one case) until adequate coverage of the balloon was confirmed at CT on limited scans obtained every 2–3 minutes as needed. Results of previous animal studies from our laboratory have demonstrated the adequacy of this amount of time to ablate normal porcine hepatic parenchyma (16).

Following completion of the freezing process, active thawing was performed, and the probes were withdrawn. A final contrast-enhanced scan of the liver was obtained by intravenously administering iohexol 2 mL/kg (Omnipaque; Nycomed, Princeton, NJ). To maintain hemostasis, absorbable collagen fabric (Surgicel; Johnson and Johnson, Arlington, Tex) was formed into rolls and was placed down the cryoprobe sheaths, and the animals were allowed to recover. No post-recovery scans were obtained. Hounsfield unit data were gathered for the ice ball and for areas of normal liver, and the size of the ice ball and the CT-determined margins were measured for radiologic-histopathologic correlation.

Histopathologic Examination

Animals were euthanized 24–96 hours after cryoablation, and their livers were preserved by using a direct-infusion technique. Animals were first reanesthetized and were given an intravenous bolus of 2,000 U of heparin. They were then sacrificed with an intravenous overdose of pentobarbital sodium and phenytoin sodium (Beuthanasia-D; Schering-Plough Animal Health, Kenilworth, NJ).

The abdomen was immediately explored for signs of hemorrhage or other pathologic condition. The distal portal vein, the hepatic artery, and the infrahepatic inferior vena cava were ligated, and the suprahepatic inferior vena cava was exposed and was lacerated. The intrahepatic portal vein was cannulated and was infused with 1,000 mL of 10% neutral buffered formalin. The liver was then removed en bloc, was immersed for at least 24 hours in formalin, and was sliced in approximately 5-mm sections in the transverse plane. The overall size and shape of the cryolesion were recorded in three dimensions, and six margins were obtained between the balloon and the rim of necrosis. Representative areas were harvested for microscopic analysis, were fixed in paraffin, and were stained with hematoxylin-eosin.

Statistics

Hounsfield unit means were calculated for targeted and untargeted areas of liver and were compared by using a paired Student t test. The diameters of the cryolesions as measured at CT and at histopathologic examination were also compared with a paired Student t test.

RESULTS

Animals

All animals survived to complete the entire protocol without apparent complication. In fact, on awakening from anesthesia, all animals resumed normal eating, defecation, and urination. Postmortem abdominal exploration did not reveal evidence of intraperitoneal hemorrhage in any case. However, all livers showed evidence of small subcapsular hematomas at the puncture site. In two cases, a small hematoma had formed between the thin porcine liver lobes where the probe had passed completely through

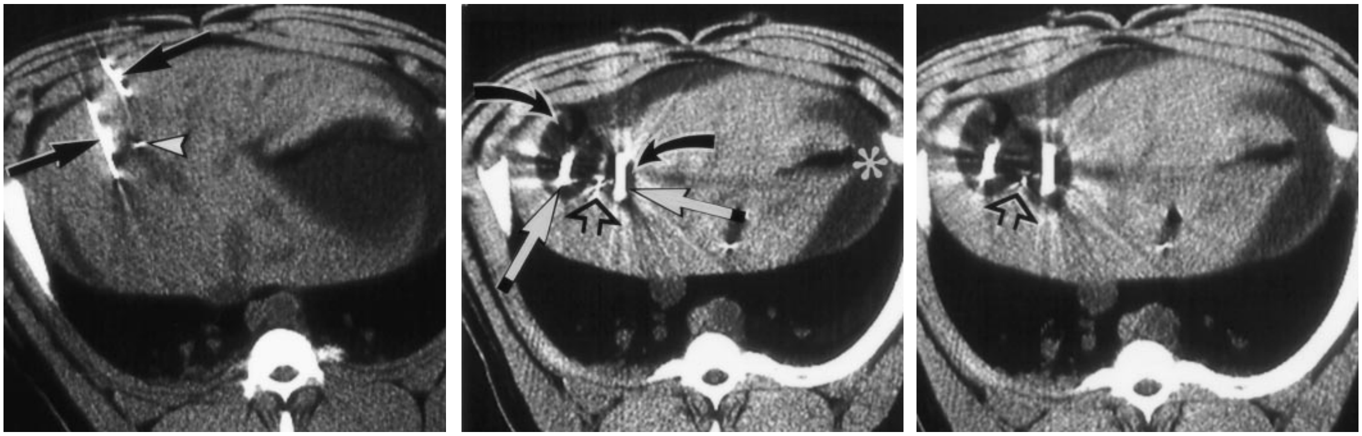

a. b. c.

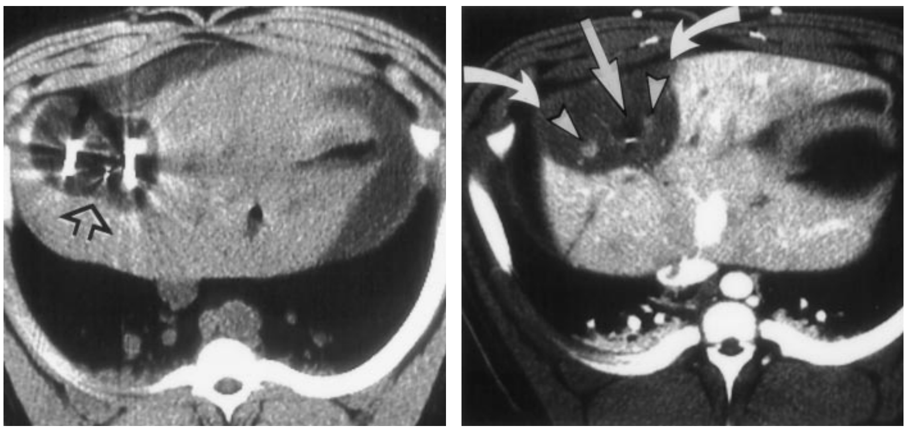

d. e.

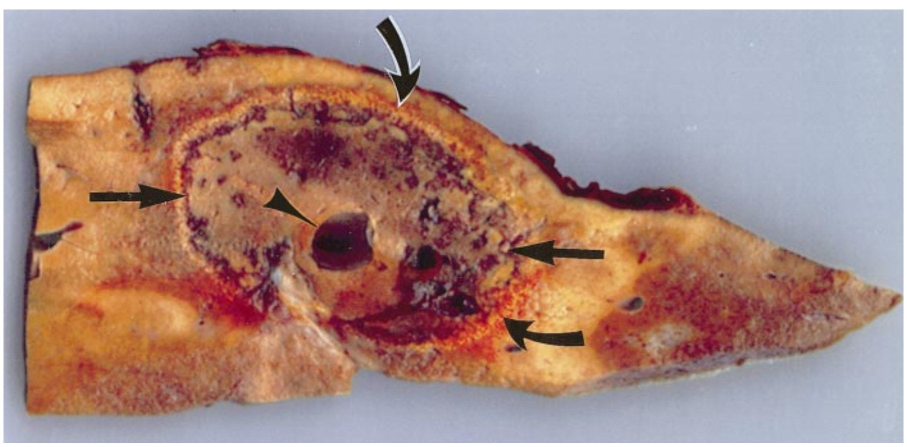

f.

Figure 1. **(a–e)** CT images demonstrate percutaneous cryoablation procedure. **(a)** Guide wires (arrows) are placed on either side of an agar-filled balloon that functions as a target. The small metal balloon valve is a bright spot (arrowhead) surrounded by the lower-attenuation agar. **(b)** Cryoablation at 2 minutes into the freezing process. The guide wires have been replaced by cryoprobes (straight solid arrows) by using the Seldinger technique. Note the markedly hypoattenuating appearance of the ice balls (curved arrows) with smooth, clearly demarcated borders. Cryoprobes exhibit some beam-hardening artifact, but not enough to interfere with the monitoring of tissue destruction. The target balloon is not yet covered by ice because of the cleft between the two ice balls (open arrow). Ascitic fluid (*) surrounding the liver is saline solution from intraabdominal irrigation intended to insulate the diaphragm and the thoracic structures from potential freezing damage. **(c)** Image obtained at 5 minutes depicts the cleft (arrow) in the progressing cryolesion. **(d)** Image obtained at 20 minutes shows that ice has filled the cleft (arrow) and has covered the lesion and an ablative margin. **(e)** Postprocedure contrast material–enhanced image demonstrates the ablated zone of the liver. Note the high-attenuation cellulose packing material in the probe tracts (arrowheads). The portion of the liver peripheral to the cryolesion has been temporarily devascularized (curved arrows) by the ice ball and does not enhance with contrast material. The agar lesion (straight arrow) is still evident within the cryolesion. **(f)** Gross axial section corresponding to the CT images. The cryolesion (straight arrows) is ovoid with a smooth, clearly demarcated border and appears deep red. The targeted agar lesion (arrowhead) and an ablative margin have been completely encompassed. The cryolesion is bordered by a thin white rim of tissue (curved arrows) corresponding to infiltration by leukocytes and is surrounded by normal-appearing parenchyma.

the most anterior lobe and into the posterior lobe, which resulted in incomplete tamponade of the probe tract.

CT Scans

During probe placement, the cryoprobes caused moderate beam-hardening artifact that would have posed limitations on a diagnostic scan, but the artifact did not interfere with monitoring of the cryoablation. In one case, a probe failed (this single-use probe had been used on multiple occasions), which resulted in an apparent positive margin at CT (Fig 2). Due to scanner time limitations, the probe was not replaced.

The ice balls were markedly hypoattenuating (1.0 HU ± 20.7) when compared with normal unenhanced liver (48.2 HU ± 6.3, $P < .05$), and the progression of the ice-ball margin could be readily visualized during the course of the freezing process. The ice ball was elliptic with a smooth, well-defined border. Where the

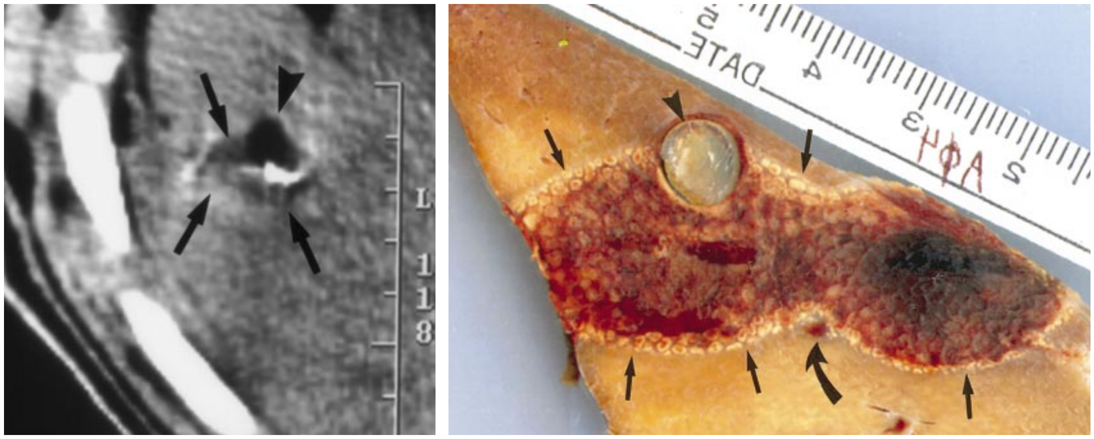

a. **b.**

Figure 2. **(a)** Positive margin identified at CT. CT image shows the target balloon (arrowhead) clearly is not covered by the small hypoattenuating cryolesion (arrows). In this case, failure of the anterior probe because of overuse of single-use probes in our animal laboratory resulted in an ice ball of insufficient size. Because of time constraints, a new probe was not placed. **(b)** Pathologic examination of the corresponding section confirms the positive margin. Area of frozen liver (straight arrows) is not large enough to encompass the anterior margin of the balloon (arrowhead). Note the invagination of the ice ball by a patent vessel (curved arrow). (Scale is in centimeters. Image is oriented to allow correlation to **a**, irrespective of ruler orientation.)

ice balls merged, no zone of transition between ice balls was identified at CT. The mean diameter of the cryolesion was 3.4 cm ± 1.2 (range, 1.5–5.4 cm).

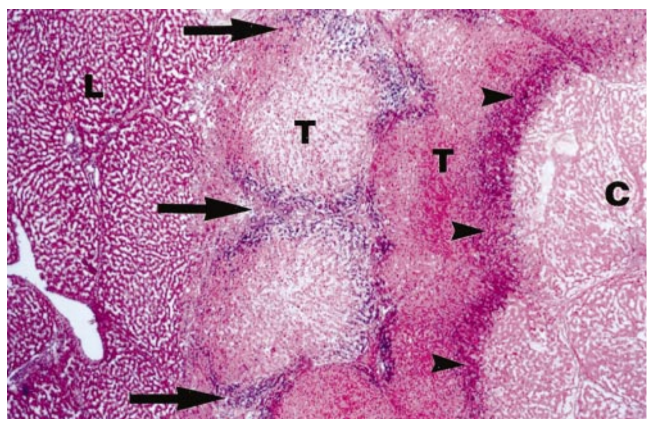

Figure 3. Histologic view of cryolesion border, from left to right: normal liver (*L*), transition zone between normal liver and cryoablated liver (*T*), and cryolesion (*C*). The normal liver (*L*) contains cells with healthy nuclei and readily identifiable lobules. At the outer edge of the cryolesion transition zone (*T*) are calcified, necrotic hepatocytes (arrows). Inner border of the transition zone (*T*) contains degenerating polymorphonuclear leukocytes (arrowheads). The transition zone defined by these two lines corresponds to the thin white rim at gross inspection. Within the cryolesion (*C*), tissue demonstrates complete homogeneous necrosis corresponding to the area of deep red hemorrhage seen at gross inspection. Individual cellular details are ablated, and no nuclei are present. (Hematoxylin-eosin stain; original magnification, ×20.)

Pathologic Findings

In liver sections, the cryolesion was seen as a dark red, elliptic zone that corresponded well to the CT depiction of ice-ball size and shape. The mean diameter was 3.2 cm ± 0.9 (range, 1.3–4.5 cm; $P > .50$ [for the mean diameter at gross examination vs the mean diameter at CT]). The rim of the cryolesion was smooth and regular in every case. The rim of the cryolesion was surrounded by a thin white zone of tissue measuring less than 1.0 mm. Beyond this zone, the lesion was surrounded by normal-appearing liver.

Histologic Findings

The interior of the cryolesion was a homogeneous distribution of necrotic cells. Discrete cellular architecture was not discernible; ghostlike cells appeared in a trabecular pattern and in lobules. Nuclei, when present, demonstrated pyknosis and karyorrhexis. The border of the cryolesion, which appeared white at gross inspection, microscopically contained degenerating polymorphonuclear leukocytes. Beyond this border, a zone of calcified necrotic hepatocytes was present. Outside the cryolesion, cells appeared undamaged with normal cellular borders and nuclei, lobular patterns, and blood vessels (Fig 3).

Margins

Because of the abrupt transition between necrotic and normal liver, it was possible to precisely measure the margins between the balloon and the necrotic area. This could be considered analogous to the surgical margins described in liver resection specimens. Only one of nine (11%) balloons had a positive margin. This was the case with probe failure, and the positive margin had been predicted at CT. The overall mean margin was 1.7 cm (range, 0–4.1 cm). Margins are presented in the Table.

Cryosurgical Margins

Margin	No. of Measurements (n = 54)
≤0 mm	1 (2)*
1–9 mm	15 (28)
≥10 mm	38 (70)

Note.—The number in parentheses is the percentage. Measurements were recorded in six locations per lesion.
* In the case with probe failure.

DISCUSSION

Traditionally, cryoablation has been limited by a danger of bleeding when accessing the liver during laparotomy or laparoscopy (22,23). Unlike radio-frequency ablation or laser photocoagulation, cryoablation does not cauterize tissue, which can cause bleeding from the probe tract or from cracking of the liver surface during thawing (24,25). This complication is usually seen immediately after the ice ball has thawed. In this study, we have demonstrated the feasibility of performing percutaneous cryoablation without causing serious bleeding.

Bleeding from the probe tract was limited by using small probes (2.4 and 3.0 mm), which are available with this argon gas–based system, as well as by using clotting material that was inserted into the cryoprobe tract. Although this strategy works well in the pig liver, insertion of clotting material down a longer tract in humans may be more technically difficult. A dedicated device to plug the probe tract would make this procedure technically easier, faster, and safer. Performing percutaneous cryoablation with larger-diameter cryoprobes may be technically feasible, but this would likely increase the chance of bleeding from the probe tract. We anticipate the development of smaller probes (2.0 mm or smaller), which should further decrease the bleeding risk.

Cracking of the liver surface has been described with open cryoablation (17, 21,24,25), but it was not encountered in this study. The absence of cracking in our subjects may be related to the percutaneous approach, which did not expose the cryolesion at the liver surface to air. Previous experimental data have demonstrated an increased risk of cracking at large ice ball-air interfaces, such as those seen with open cryoablation, whereas deep lesions and those covered with a fabric mesh were unlikely to crack and to cause serious bleeding (26).

Even if cracking were to take place, data from the trauma literature, which describes situations in which many hepatic lacerations are treated conservatively, suggest that a small crack would not necessarily require laparotomy, as long as the subject remained hemodynamically stable (27). However, the potential dangers of percutaneous cryoablation in humans will not be completely known until clinical trials are undertaken, and the risk of bleeding should be carefully considered prior to application of this procedure in patients. We are aware of a single case in which percutaneous cryoablation was performed in a patient who was not a surgical candidate (Onik GM, oral communication, 1998). The procedure was guided with US without bleeding or other complications, and the patient was rapidly discharged from the hospital in excellent condition.

Percutaneous cryoablation is limited by the potential for collateral damage to organs proximal to the liver. During open cryoablation, the intestine and diaphragm are protected with insulating material. The inability to protect these organs will limit the use of percutaneous cryoablation to lesions that are deep in the liver parenchyma or remote from vital extrahepatic structures.

However, the most important consideration in the percutaneous application of any ablative technology is whether the advantages of a percutaneous approach outweigh the possible disadvantages of missing more lesions because intraoperative inspection and US would not be performed. Intraoperative US reveals 7%–35% more lesions than any preoperative imaging modality, and its increased specificity for characterizing small lesions, such as cysts, helps in the appropriate triage of patients for treatment (28–30).

Until preoperative imaging techniques become more accurate, performing percutaneous tumor ablation without intraoperative US will virtually guarantee that a sizable subset of patients with metastases will be under- or overtreated. Although this may be acceptable for certain patients who are not surgical candidates because of coexistent morbid conditions, it raises questions about the broad application of this and other percutaneous ablative technologies.

The ablative margins and ice-ball size encountered in this study appear adequate for the ablation of small tumors. Larger tumors in human livers will require more extensive tissue destruction and will require the use of additional probes. The thin, multilobar configuration of pig livers prevented the creation of larger ice balls and larger margins because of the increased risk of collateral damage. However, even with these limitations, we believe that the margins reported in this study are reasonable when compared to margins reported in the surgical data. The stated goal of hepatic resection is to attain a 1.0-cm surgical margin. However, only approximately 20% of resection specimens meet this standard (31–33). The positive margin in our series was due to a probe failure brought on by repeated use of a single-use probe in our laboratory. The probe was not replaced because of restrictions in the hours that CT scanners are available for use with animals. In humans, most cryoprobes are single use only, and probe failure is rare.

Performing cryoablation with CT guidance has advantages over performing cryoablation with guidance from magnetic resonance (MR) imaging. Experience with CT-guided procedures is widespread, and virtually any modern CT scanner should suffice for guiding cryoablation. The cryoablation equipment currently available for clinical use would not have to be modified extensively for use with CT, although less attenuating probe material could decrease the beam-hardening artifact. Major modifications in probe and tubing materials are necessary for use proximal to magnets (34). Most of the lesions treated with cryoablation will have been diagnosed at CT, so there should be no difficulty in locating and in puncturing the same lesions. The ice ball is well depicted at CT, which adds to the confidence that the lesion has been adequately treated.

Newer helical units with rapid reconstruction times are particularly suited for guiding cryoablation because of their real-time or CT fluoroscopic capability that can be used during needle and probe placement. In addition, rapid two-dimensional multiplanar reconstructions are now possible, and, as they are with MR imaging, these can be used to help avoid damaging structures, such as the diaphragm, that are oriented in the transverse plane. Disadvantages in the use of CT include the use of ionizing radiation; the use of small gantry sizes, which could limit the use of this procedure in large patients; slow reconstruction times in some scanners; and difficulty in depicting the tumor on noncontrast scans in some cases. The main disadvantage of CT, compared with MR imaging, is its inability to measure temperature gradients within the ice ball (35).

CT appears to have several advantages over US in the guidance of percutaneous cryoablation. As stated previously, radiologists are comfortable with performing interventional procedures with CT guidance, there is a widespread availability of CT scanners, and advances in CT technology are moving it closer to being a real-time guidance modality. Most important, the entire ice ball, including the deep margin, is well depicted at CT. In contrast, US depicts only the anterior edge of the ice ball because of the inability of sound waves to penetrate ice (20,36,37). This is not a serious limitation during intraoperative use because the US probe can be moved to almost any location on the liver, including the inferior and posterior surfaces, while an adequate sonic window is still maintained (29,36).

In addition, the inability to visualize a tumor while performing cryoablation increases the confidence that the tumor is completely engulfed by the ice ball. However, during percutaneous cryoablation, it may not be possible to find an adequate sonic window in which to visualize all of the margins of the ice ball because of intervening ribs, bowel gas, and subcutaneous tissues. The end result is suboptimal visualization of the entire ice ball, the margin of ablation, and the surrounding structures.

These limitations may contribute to the large number of local recurrences seen with some ablation techniques that are guided solely by percutaneous US rather than by intraoperative US (9–11). The major disadvantage of CT, as compared with US, is its relatively increased expense in terms of equipment and time and the lack of true real-time guidance for needle and probe placement. These limitations can be partially overcome with the combined use of CT and US, as demonstrated in this study, as well as by advances in CT technology.

Practical application: Percutaneous cryoablation of the liver is technically feasible and did not cause serious bleeding in this animal model. CT monitoring of the ice ball provides images that accurately map tissue necrosis, allows adequate visualization of surrounding intra- and extrahepatic structures, and is widely available. We predict that with minimal probe reconfiguration and with a better hemostatic device, this technology should be applicable to humans. However, the lack of surgical exploration and intraoperative US inherent in any percutaneous ablation procedure will lead to decreased sensitivity for lesion detection and decreased specificity in lesion characterization. This could increase the number of patients who are either under- or overtreated until preoperative imaging modalities approach the sensitivity and specificity of intraoperative US.

Acknowledgments: The authors thank Margaret A. Rankin, BS, and Alan H. Rappe, RTR, for assistance with animal care; Carrie E. Poole for assistance with manuscript preparation; and Douglas O. Chinn, MD, Wilson S. Wong, MD, and Gary M. Onik, MD, for inspiration and advice concerning the technical aspects of this study and experimental design.

References

1. Landis SH, Murray T, Bolden S, Wingo PA. Cancer statistics, 1999. CA Cancer J Clin 1999; 49:8–31.
2. Asbun HJ, Hughes KS. Management of recurrent and metastatic colorectal carcinoma. Surg Clin North Am 1993; 73:145–166.
3. Weiss L, Grundmann E, Torhorst J, et al. Haematogenous metastatic patterns in colonic carcinoma: an analysis of 1541 necropsies. J Pathol 1986; 150:195–203.
4. Hughes K, Scheele J, Sugarbaker PH. Surgery for colorectal cancer metastatic to the liver: optimizing the results of treatment. Surg Clin North Am 1989; 69:339–359.
5. Fong Y, Kemeny N, Paty P, Blumgart LH, Cohen AM. Treatment of colorectal cancer: hepatic metastasis. Semin Surg Oncol 1996; 12:219–252.
6. Asbun HJ, Tsao JI, Hughes KS. Resection of hepatic metastases from colorectal carcinoma: the registry data. Cancer Treat Res 1994; 69:33–41.
7. Hughes KS, Simon R, Adson MA, et al. Resection of the liver for colorectal carcinoma metastases: a multi-institutional study of indications for resection. Surgery 1988; 103:278–288.
8. Ravikumar TS. Interstitial therapies for liver tumors. Surg Oncol Clin N Am 1996; 5:365–377.
9. Livraghi T, Goldberg SN, Monti F, et al. Saline-enhanced radio-frequency tissue ablation in the treatment of liver metastases. Radiology 1997; 202:205–210.
10. Solbiati L, Ierace T, Goldberg SN, et al. Percutaneous US-guided radio-frequency tissue ablation of liver metastases: treatment and follow-up in 16 patients. Radiology 1997; 202: 195–203.
11. Rossi S, Di Stasi M, Buscarini E, et al. Percutaneous RF interstitial thermal ablation in the treatment of hepatic cancer. AJR 1996; 167: 759–768.
12. Amin Z, Donald JJ, Masters A, et al. Hepatic metastases: interstitial laser photocoagulation with real-time US monitoring and dynamic CT evaluation of treatment. Radiology 1993; 187:339–347.
13. Nolsøe CP, Torp-Pedersen S, Burcharth F, et al. Interstitial hyperthermia of colorectal liver metastases with a US-guided Nd-YAG laser with a diffuser tip: a pilot clinical study. Radiology 1993; 187:333–337.
14. Yang R, Sanghvi NT, Rescorla FJ, Kopecky KK, Grosfeld JL. Liver cancer ablation with extracorporeal high-intensity focused ultrasound. Eur Urol 1993; 23(suppl 1):17–22.
15. Adams JB, Moore RG, Anderson JH, Strandberg JD, Marshall FF, Davoussi LR. High-intensity focused ultrasound ablation of rabbit kidney tumors. J Endourol 1996; 10:71–75.
16. Weber SM, Lee FT Jr, Warner TF, Chosy SG, Mahvi DM. Hepatic cryoablation: US monitoring of extent of necrosis in normal pig liver. Radiology 1998; 207:73–77.
17. Kane RA. Ultrasound-guided hepatic cryosurgery for tumor ablation. Semin Intervent Radiol 1993; 10:132–142.
18. Wong WS, Patel SC, Cruz FS, Gala KV, Turner AF. Cryosurgery as a treatment for advanced stage hepatocellular carcinoma. Cancer 1998; 82:1268–1278.
19. Lee FT Jr, Mahvi DM, Chosy SG, et al. Hepatic cryosurgery with intraoperative US guidance. Radiology 1997; 202:624–632.
20. Ravikumar TS. The role of cryotherapy in the management of patients with liver tumors. Adv Surg 1996; 30:281–291.
21. Onik GM, Atkinson D, Zemel R, Weaver ML. Cryosurgery of liver cancer. Semin Surg Oncol 1993; 9:309–317.
22. Curley SA, Davidson BS, Fleming RY, et al. Laparoscopically guided bipolar radiofrequency ablation of areas of porcine liver. Surg Endosc 1997; 11:729–733.
23. Patterson EJ, Scudamore CH, Buczkowski AK, Owen DA, Nagy AG. Radiofrequency ablation in surgery. In: Surgical technology international VI: international development in surgery and surgical research. San Francisco, CA: Universal Medical, 1996.
24. Onik G, Rubinsky B, Zemel R, et al. Ultrasound-guided hepatic cryosurgery in the treatment of metastatic colon carcinoma: preliminary results. Cancer 1991; 67:901–907.
25. Ravikumar TS, Kane R, Cady B, Jenkins R, Clouse M, Steele G Jr. A 5-year study of cryosurgery in the treatment of liver tumors. Arch Surg 1991; 126:1520–1524.
26. Dutta P, Montes M, Gage AA. Large volume freezing in experimental hepatic cryosurgery: avoidance of bleeding in hepatic freezing by an improvement in the technique. Cryobiology 1979; 16:50–55.
27. Croce MA, Fabian TC, Menke PG, et al. Nonoperative management of blunt hepatic trauma is the treatment of choice for hemodynamically stable patients: results of a prospective trial. Ann Surg 1995; 221:744–755.
28. Kane RA, Hughes LA, Cua EJ, Steele GD, Jenkins RL, Cady B. The impact of intraoperative ultrasonography on surgery for liver neoplasms. J Ultrasound Med 1994; 13:1–6.
29. Kruskal JB, Kane RA. Intraoperative ultrasonography of the liver. Crit Rev Diagn Imaging 1995; 36:175–226.
30. Soyer P, Elias D, Zeitoun G, Roche A, Levesque M. Surgical treatment of hepatic metastases: impact of intraoperative sonography. AJR 1993; 160:511–514.
31. Cady B, Stone MD, McDermott WV, et al. Technical and biological factors in disease-free survival after hepatic resection for colorectal cancer metastases. Arch Surg 1992; 127:561–569.
32. Jamison RL, Donohue JH, Nagorney DM, Rosen CB, Harmsen WS, Ilstrup DM. Hepatic resection for metastatic colorectal cancer results in cure for some patients. Arch Surg 1997; 132:505–511.
33. Scheele J, Stang R, Altendorf-Hofmann A, Paul M. Resection of colorectal liver metastases. World J Surg 1995; 19:59–71.
34. Tacke JA, Speetzen R, Adam GB, VanVaals JJ, Rau G, Gunther RW. MR-guided interstitial cryotherapy with a liquid nitrogen cooled cryoprobe (abstr). Radiology 1997; 205(P):200.
35. Gilbert JC, Rubinsky B, Wong STS, Brennan KM, Pease GR, Leung PP. Temperature determination in the frozen region during cryosurgery of rabbit liver using MR image analysis. Magn Reson Imaging 1997; 15:657–667.
36. Onik G, Cooper C, Goldberg HI, Moss AA, Rubinsky B, Christianson M. Ultrasonic characteristics of frozen liver. Cryobiology 1984; 21:321–328.
37. Weber SM, Lee FT Jr, Chinn DO, Warner T, Chosy SG, Mahvi DM. Perivascular and intralesional tissue necrosis after hepatic cryoablation: results in a porcine model. Surgery 1997; 122:742–747.